

# Walking Pole Gait to Reduce Joint Loading post Total Knee Arthroplasty: Musculoskeletal modeling Approach

Oishee Mazumder<sup>1</sup>, Murali Poduval<sup>1</sup>, Avik Ghose<sup>1</sup> and Aniruddha Sinha<sup>1</sup>

**Abstract**—Excessive knee contact loading is precursor to osteoarthritis and related knee ailment leading to knee arthroplasty. Reducing contact loading through gait modifications using assisted pole walking offers noninvasive process of medial load offloading at knee joint. In this paper, we evaluate the efficacy of different configuration of pole walking for reducing contact force at the knee joint through musculoskeletal (MSK) modeling. We have developed a musculoskeletal model for a subject with knee arthroplasty utilizing in-vivo implant data and computed tibio-femoral contact force for different pole walking conditions to evaluate the best possible configuration for guiding rehabilitation, correlated with different gait phases. Effect of gait speed variation on knee contact force, hip joint dynamics and muscle forces are simulated using the developed MSK model. Results indicate some interesting trend of load reduction, dependent on loading phases pertaining to different pole configuration. Insights gained from the simulation can aid in designing personalized rehabilitation therapy for subjects suffering from Osteoarthritis.

## I. INTRODUCTION

Joint contact dynamics is an integral evaluation parameter to estimate the loading effect on weight bearing joints in any musculoskeletal (MSK) disorder [1]. Knee joint is the largest weight bearing joint facilitating locomotion. Being such a crucial joint, knee related injuries and ailments are the most common MSK disorders, ranging from strained ligament, cartilage tear, traumatic injury, sports injury, age related degeneration and Osteoarthritis (OA) [2]. There has been considerable study on prevalence of OA lately, accelerated by the fact that the disease have started showing high prevalence in younger population group, due to obesity and lifestyle changes [3]. Knee OA accounts for 80% of OA burden worldwide and the only effective mode of treatment is knee arthroplasty (TKA) at advanced stage of the disease, adding substantial cost and recovery burden [4]. Additionally, knowledge of the loading conditions and contact forces in MSK system forms the basis for understanding a wide range of biomechanical processes related to injury, wear and tear, adaptation to orthopedic treatment, rehabilitation and optimal implant design for TKA [5].

Altered gait kinematics is an effective way of redistributing joint loads through training and rehabilitation therapy. Modifying gait results in reduction in external knee adduction moment, which is believed to reduce tibiofemoral loading [6]. Various gait modification techniques like walking at reduced speed, toe-out gait, medial thrust gait, increased trunk sway

and assisted walking with pole supports have been reported to be efficient in reducing joint loads and contact forces [7]. Modified gaits leads to decrease in adduction moments but what fraction of the adduction moment contributes to contact loading and how the load varies with load distribution during gait phases are yet to be standardized [8]. Similarly for pole walking, although it is established that pole walking aids in lower limb load reduction, effect of different pole walking techniques on the MSK system as a whole with additional gait variation is still an active area of research [9].

Computational modeling has become an integral component of predictive analysis and knowledge discovery in MSK domain [10]. MSK models have been used to estimate tibio-femoral contact forces by integrating Finite element models, gait models and contact dynamics [11]. Contact forces are usually estimated through muscle force estimation combined with inverse dynamics loading [12]. There has been prior work on knee contact force estimation using muscle force simulation and then combining the force estimates with ground reaction forces and hertzian contact model[13]. In some cases, a spring based contact model is used to compute node to surface knee contact forces using inverse dynamics along with computed muscle control algorithm to estimate muscle force [14]. Knee contact forces can also be predicted without contact models, based on muscle forces estimation using pseudo-inverse method and parameter reduction strategy [15]. In spite of advancement in computational modeling, the main challenge remains in validating these models with measured clinical data. An initiative in the form of Grand challenge has made in vivo knee contact force available from subject with an instrumented knee [16]. Availability of in-vivo data has revolutionized the use and applicability of the computational MSK models for predicting contact dynamics and aiding in surgical and functional rehabilitation treatments of the MSK disorders.

In this paper, we present a lower limb musculoskeletal model developed in OpenSim platform, incorporating a prosthetic implant knee along with associated muscle and ligament to assess and estimate tibio-femoral contact loads along with knee and hip joint loading and muscle force distribution for different gait configurations. Gait configurations are normal walking and four different bilateral pole walking conditions naming, Long Normal (LN), Long Wide (LW), Short Normal (SN) and Short Wide (SW) configuration. Through the proposed model, we evaluate both knee and hip joint loading and muscle distribution force during the stance phase; specifically at point of initial contact, loading, mid-stance and terminal stance, to evaluate loading dynamics

<sup>1</sup>Oishee Mazumder, Murali Poduval, Avik Ghose and Aniruddha Sinha are with TCS Research, Tata Consultancy Services Ltd, India.

Email:oishee.mazumder@tcs.com, murali.poduval@tcs.com,  
avik.ghose@tcs.com, aniruddha.s@tcs.com

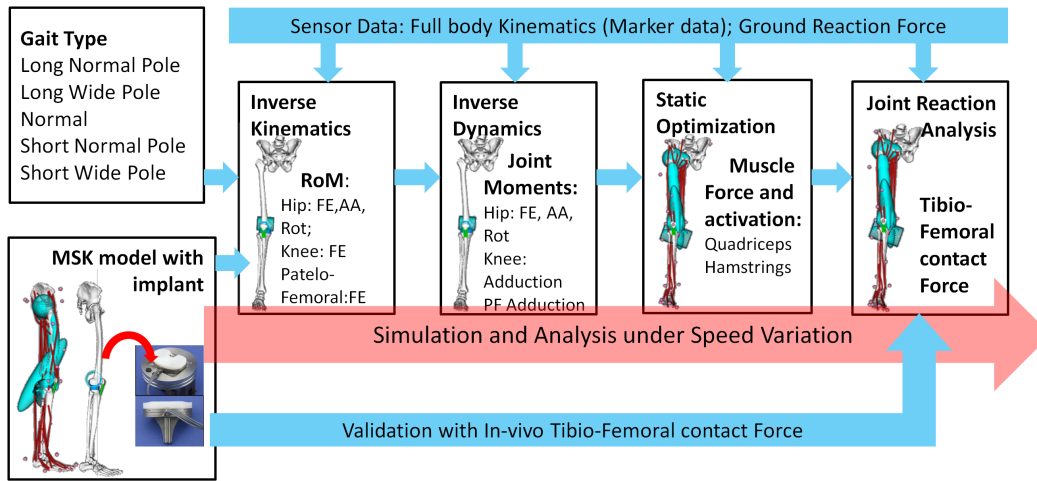


Fig. 1: Schematic work-flow; FE: Flexion-Extension, AA: Adduction-abduction, Rot:Rotation

with motion and also with speed variation. Key contribution of this paper are:

- Musculoskeletal model to predict tibio-femoral contact force along with hip and knee joint loading for normal walking and four different walking pole configuration.
- Simulate the effect of speed variation in loading dynamics and muscle force distribution.

## II. METHODOLOGY

Musculoskeletal model presented in this paper mimics the lower limb of a subject with force measuring knee replacement device. Model is scaled as per subject's anthropomorphic data and the implant model is integrated with the subject's tibio-femoral joint. We compute inverse kinematics to derive joint kinematics from marker data, inverse dynamics to compute joint moments, static optimization for muscle force optimization and joint reaction analysis for contact force estimation. Estimated contact forces are compared with the in-vivo data for validation for all the gait cases under consideration. The computational pipeline is next simulated for walking with increased speed and all the parameters were recomputed for evaluation. A schematic of the computational work-flow is presented in Fig.1.

### A. Implant Evaluation Data

Subject data and implant specifications were adapted from 4th Grand-challenge data [16]. Subject under study had a force measuring knee implant at right knee. Implantation was due to primary knee osteoarthritis. Subject (male, 83 years, weight: 68 Kg, height: 1.7 m) performed overground gait and pole walking at self selected walking speed of around 1.23 m/sec. Kinematics data were recorded using 8 VICON camera system using 64 markers from modified Cleveland Clinic marker set. External ground reaction force during walking were recorded using 3 AMTI force plates. Implant was a custom tibial prosthesis with generation I implant design, instrumented with 4 uniaxial force transducers (load cell) to measure compressive force, implanted at four corners

of the tibial tray.

For walking pole gait, subject used two walking poles with rubber tip (Leki Makalu tour trekking poles) and walked at a self selected speed (1.23 m/sec). Subject was instructed to place the contralateral pole on the ground opposite his stance leg heel at the instant of heel strike. 5 trials for 5 such gait patterns: normal (without pole) and 4 pole walking conditions were performed. 'Long' pole refers to standard hiking pole height and 'short' refers to reduction of height by 10%. 'Normal' configuration refers to holding the pole at 90 degree elbow flexion angle with the pole tip placed vertical to the ground, while 'wide' refers to placing the poles at a wide width by externally rotating the shoulder at comfortable range.

Medial and lateral contact forces were calculated from the implants force transducer data using regression equation[17]:

$$F_M = C_1 F_{AM} + C_2 F_{PM} + C_3 F_{AL} + C_4 F_{PL}$$

$$F_L = (1 - C_1) F_{AM} + (1 - C_2) F_{PM} + (1 - C_3) F_{AL} + (1 - C_4) F_{PL} \quad (1)$$

where  $F_M$  and  $F_L$  are the medial and lateral contact force,  $C_1(0.9871), C_2(0.9683), C_3(0.0387), C_4(0.0211)$  are the regression coefficients and the subscripts A, M, P, and L represent the anterior, medial, posterior, and lateral force transducers.

### B. Musculoskeletal Model

The developed MSK model replicates the structural component of the subject with prosthetic knee, developed in OpenSim environment. MSK model was modified from an existing lower limb gait model [18]. We incorporated the implant geometry of the tibial prosthesis along with the e-knee (instrumented tray) and modified the base model to match kinetic and kinematic constraints of the data set. The improvised model consists of pelvis joint, hip joint, knee joint, patelofemoral joint, ankle joint, subtalar and metatarsophalngeal joint, all with six degree of freedom, 3 rotational (R) and 3 translational (T). The implant geometries

were linked as femoral component weld and tibial tray weld. Although the knee and patelofemoral joint is structurally provided with 3R, 3T motion, only flexion motion (motion along sagittal plane) was enabled, others were locked. The model was driven by 44 muscle units, divided into hip adduction-abduction, flexion, extension and rotation, knee flexion-extension, ankle dorsiflexion-plantar-flexion, evertor-inverter muscle group. Along with the muscle units, knee structure was also coupled with 3 main ligament structures, naming Anterior cruciate ligament, Posterior Cruciate Ligament (PCL) and Fibular Collateral Ligament (FCL). All the ligaments were modeled as nonlinear elastic bundles, tension being the function of its length or strain. Developed MSK model is shown in Fig.2a.

Developed model was used to replicate different walking dynamics of the subject with instrumented knee. These involved conversion of raw motion data to OpenSim compatible formats, synchronizing marker (22 markers on MSK model) and ground reaction force data, registering measurement data to OpenSim model and model scaling. Inverse kinematics tool was used to compute joint trajectories from marker data by minimizing error between measured marker positions and corresponding markers on the model. Joint torques were calculated using the inverse dynamics engine, taking in to account the joint trajectory and the measured ground reaction force. Joint torques were calculated as:  $\ddot{q} = [M(Q)]^{-1} \{ \tau + C((q, \dot{q}) + G(q) + F) \}$  where,  $\ddot{q}$  is the acceleration due to joint torque  $\tau$ ,  $M$  is the mass matrix,  $C$  and  $G$  are the Coriolis and gravity component and  $F$  is any external force applied to the model.

For muscle force estimation, static optimization framework was used. Muscle forces were generated using ‘Thelen’ muscle actuator, where, muscle torque is expressed as a function of three factors: activation value ( $a$ ), normalized length of the muscle unit ( $l$ ), and normalized velocity of the muscle unit ( $\dot{l}$ ). Muscle torque component ( $\tau_m$ ) is calculated as follows:  $\tau_m = [R(q)]f(a, l, \dot{l})$ ,  $[R(q)]$  is the moment arm [19]. As the model is a reduced order model capturing the dynamics of instrumented leg only, residual reduction algorithm was used to model external actuator to append for missing muscle forces and adjust the ground reaction forces and body segment accelerations.

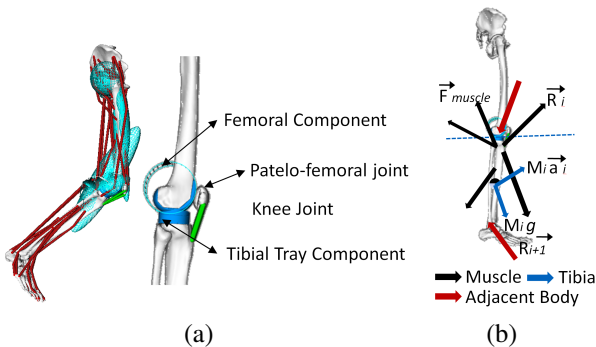


Fig. 2: a) Lower limb MSK model with implant; b) Free body diagram to calculate tibiofemoral contact force

### C. Contact Force Estimation

Net loading force or contact force are generated due to combination of forces and moments acting at the joint due to various muscles, ligaments and adjacent joints. Inverse dynamics module calculates the net generalized forces in the model, while static optimization provides an estimate of optimal muscle forces required to balance the moment generated by the associated joints. However, summing them up does not represent contact force between two bodies. The Joint Reaction analysis module calculates the resultant forces and moments generated at the joint structure, in response to all motions and forces in the model including muscles, external forces and actuators [20]. Joint Reaction analysis calculates joint loads in a post processing step, where a recursive procedure is followed for each joint. This is analogous to constructing a free body diagram for each rigid body and resolving the point load that must be applied to the joint to balance the forces and motions of the body. For calculating knee contact force (tibiofemoral contact force), motion between femur and tibia can be described by splines that couple the rotations and translations of the knee and net load can be calculated as a point load acting on the tibial plateau. Compressive tibiofemoral force for gait cycle can be calculated using the Newton-Euler equation on the free body diagram (Fig.2b):

$$\vec{R}_i = M_i \vec{a}_i - (\sum \vec{F}_{muscle} + \sum \vec{F}_{external} + \vec{R}_{i+1}) \quad (2)$$

where,  $R_i$ ,  $R_{i+1}$  is the force from femur on tibia and foot on tibia respectively,  $M_i$  is the inertial matrix for tibia,  $a_i$  is the six dimensional angular and linear acceleration of the tibia,  $F_{muscle}$  and  $F_{external}$  are the equivalent muscle force and external actuator or gravity force.

## III. RESULT AND DISCUSSION

While there are numerous instances of evaluating knee adduction moment (KAM) for OA progression, contribution of associated joints on the overall gait pattern are often neglected. Compensatory movements may in fact reduce the load at the knee but may adversely affect mechanics of adjacent joints [21]-[22]. Gait biomechanics at hip joint affect medial knee loading and a decrease in hip loading along the frontal and sagittal plane have shown to lower the risk of OA progression. Taking all potential markers in to account, we computed and analyzed the response of tibiofemoral contact force, knee adduction moment, patelofemoral adduction moment, hip flexion, adduction and rotation moment along with muscle force distribution for Vastus Medialis (VM) and Vastus Lateralis (VL) muscles throughout the gait cycle (0 to 100%) and specific loading phases (0 to 100% of stance phases) for all the five gait combinations under study and for two sets of walking speed variation: S1: Self selected speed of 1.3 m/sec and S2 is the simulated speed of 2m/sec.

We computed total tibio-femoral contact force measured in-vivo (Eq.(1)), estimated tibio-femoral contact force (Eq.(2)), ground reaction force, all scaled by body-weight (BW) of the subject and report the absolute force values computed at different loading phases of gait cycle, naming

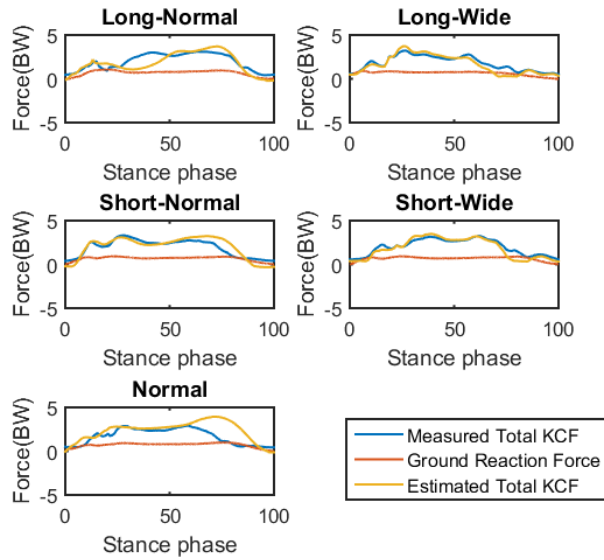


Fig. 3: Knee Contact force (KCF) and ground reaction force plots for different gait types at self selected walking speed plotted for 0 to 100% stance cycle

initial contact (0%), loading (25%), mid-stance (50%) and terminal stance (75%). Fig.3 shows the estimated tibiofemoral (TF) contact force across the stance phase for all the gait types. Estimated TF contact force matches the profile of in-vivo load measured (vector summation of medial and lateral load), with offshoots beyond terminal stance phase. TF estimated for all the gait types were in close concurrence with earlier published results [15]. Table I lists the stride time and absolute force at the contact point at different gait events along with the error percentage wrt in-vivo measurement. The errors were calculated to validate the capability of MSK model to estimate TF contact force. For the simulated speed behavior (S2), only the estimated TF value is reported.

As seen from the tabulations, estimated TF shows coherence with the measured load mostly in the initial loading and mid stance phases and this is true for all the gait variations. This reflection is due to the MSK model characterization for kinetic and kinematic constraints along with external actuator adjustments. The overall profile for all gait variations are

comparable to early publication comparing estimated load with measured in vivo loads in terms of the error band reported [23]. In terms of load variation due to gait modification, LW pole had the best reduction wrt normal gait. In our case, LW pole shows maximum load reduction in mid stance and terminal stance phases, followed by SW. Increased speed simulation (S2) showed an increase in load at all the phases wrt their S1 counterpart, however, rate of increase of load is minimal in long pole configuration (8 to 10% increase wrt to S1) while normal gait had load increased by up to 23% and short pole configurations had load increased by around 16%. This indicates that increase in speed is positively correlated with increase in load but gait supported by long poles will aid better as the gait speed increases.

We next evaluate loading at knee (Table II) with respect to the surrogate markers, naming knee adduction and patellofemoral adduction load computed through inverse dynamics and corresponding muscle force of Vastus Lateralis (VL), and Vastus medialis (VM) muscles associated with supporting knee during lateral and medial load distribution respectively. Similar to TF estimation, LW pole configuration showed maximum reduction in loading for all parameters under consideration, however, reduction around midstance is maximum. Early stance reduction with pole walking is negligible, but as the stance phase progresses, effect of pole walking in reducing joint loads become more prominent. As the moment at joints gets reduced due to pole assistance, muscle force required to support the load is also reduced.

Table III reports the hip joint loading dynamics with change in speed across different adaptive gaits. The effect of increased speed is most prominent in hip joint loading, where flexion, adduction and rotation loads all gets tremendously increased with increase in speed. The effect of pole walking is more prominent in S2, a wider pole configuration (both in long and short pole) provides reduction in hip loading wrt normal gait. It is to be noted that the values indicated in the tables are not absolute, but dependent on model parameter tuning. It is more to establish the trend of loading at respective joints. Metric loading values may change on improvising the developed model with additional joints and muscles.

To bring out the variation with speed, mean value of the joint loads over 0 to 100% of gait cycle are shown in bar plot

TABLE I: Estimated Tibiofemoral contact force for various gait types

Gait	Stride time (sec)	0% Stance	Error (%)	25% Stance	Error(%)	50% Stance	Error(%)	75% Stance	Error(%)
S1 LN	1.485	136.6	19.3	981.4	6.4	1870.2	4.1	2380	12.1
S1 LW	1.435	231.2	16.1	1897.2	6.2	1612.2	4.0	877.2	16.3
S1 NG	1.277	188.4	17.3	1994.5	5.9	1853.6	5.1	2584	14.7
S1 SN	1.301	204.1	9.6	2060.1	4.7	1887.6	3.1	1149.2	11.2
S1 SW	1.247	176.2	11.7	1339.6	4.1	1717.4	3.5	992.8	14.3
S2 LN	0.858	150.2	–	1035.6	–	1946.2	–	2573.1	–
S2 LW	0.869	242.1	–	1915.7	–	1710.6	–	1016.1	–
S2 NG	0.768	236.6	–	2205.8	–	2101.7	–	2809.2	–
S2 SN	0.779	255.4	–	2087.1	–	1967.2	–	1327.2	–
S2 SW	0.764	195.2	–	1500.4	–	1840.1	–	1005.8	–

TABLE II: Loading dynamics at knee joint for various gait types

Gait	Knee Adduction (N)				PF Adduction (N)				VM Force (N)				VL Force (N)			
	0%	25%	50%	75%	0%	25%	50%	75%	0%	25%	50%	75%	0%	25%	50%	75%
S1 LN	730.1	617.4	583.5	572.1	19.37	73.61	39.86	42.58	670.7	1050	1539	1074	1183	1812	2707	1839
S1 LW	722.9	618.4	519.3	506.3	76.91	9.33	67.95	73.07	1184	1221	1017	948.4	2147	2136	1785	1708
S1 NG	781.6	617.8	576	543.3	134.5	5.62	37.81	57.11	1082	1424	1694	721.7	1935	2462	2832	1229
S1 SN	773.8	646.4	552.8	549.4	126.2	11.15	48.29	51.37	1055	1298	1070	986.0	1940	2305	1905	1764
S1 SW	729.4	648.5	545	540.8	79.93	11.39	56.00	57.00	1081	1250	1050	985	2005	2192	1865	2192
S2 LN	710.8	634.5	528.5	508.6	32.13	89.2	61.6	22.97	513.4	998.8	1512	1686	881	1771	2659	2836
S2 LW	700.2	624.7	539.1	506.3	47.84	10.29	57.15	73.07	1011	1304	1112	886.2	1877	2316	1885	1557
S2 NG	783.0	644.1	577.9	530.6	135.6	6.032	37.81	58.61	468.1	1322	1940	1544	805.9	2298	3271	2483
S2 SN	733.6	639.9	559.6	533.1	75.31	20.68	51.83	57.12	1055	1290	1067	890	1940	2300	1875	1623
S2 SW	750.7	620.8	544.2	529.7	100.7	11.39	56.37	59.31	1050	1305	1055	890	1900	2298	1860	1600

TABLE III: Loading dynamics at hip joint for various gait types

Gait	Hip Flexion (N)				Hip Adduction (N)				Hip Rotation (N)			
	0%	25%	50%	75%	0%	25%	50%	75%	0%	25%	50%	75%
S1 LN	7.72	9.89	2.33	10.46	2.20	4.91	2.33	1.8	0.18	0.27	0.27	1.05
S1 LW	18.2	7.81	2.71	9.26	2.69	4.64	2.94	1.6	1.01	0.31	0.18	0.35
S1 NG	23.0	8.13	4.28	15.8	3.19	5.17	3.35	1.8	0.95	0.02	0.38	0.53
S1 SN	22.2	6.16	4.37	11.85	1.14	4.16	1.32	1.3	0.45	0.51	0.45	0.31
S1 SW	20.4	7.72	5.18	10.5	1.92	4.81	1.20	1.5	1.51	0.79	0.30	0.31
S2 LN	44.19	15.16	18.57	19.11	1.73	1.47	1.17	14.5	0.18	1.19	1.29	1.04
S2 LW	51.13	14.69	5.34	5.15	1.89	7.06	2.94	16.6	1.89	0.90	1.21	0.91
S2 NG	88.14	17.29	2.81	33.70	14.6	8.23	3.52	17.1	0.91	1.01	1.28	1.23
S2 SN	76.14	13.26	8.38	10.13	1.73	12.33	2.96	12.1	1.24	0.94	1.25	1.31
S2 SW	70.17	15.13	13.16	23.23	19.5	13.41	1.21	18.7	1.04	1.03	1.30	1.41

representation (Fig.4). Bar plot distribution for hip loading clearly shows the increase in load at hip joints with change in speed, whereas speed variation over the gait cycle does not show much variation for knee joints. These variations points out the need of adjacent joint analysis while treating knee related ailments.

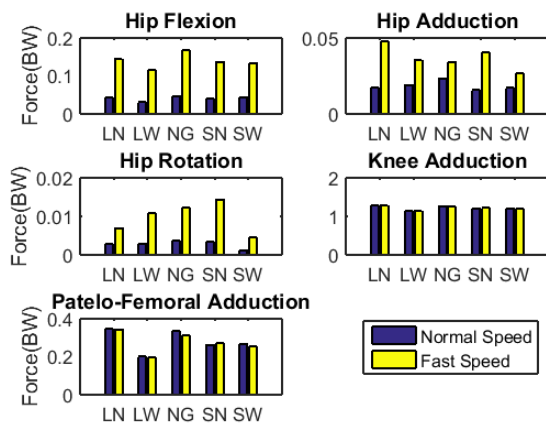


Fig. 4: Mean joint loads across 0 to 100 % gait cycle for different speed

Overall analysis indicates ‘Long-wide’ pole configuration to be most effective in reducing contact load as well as knee adduction load and hip loads and the effect is most prominent in the mid stance phase, where load bearing is maximum at

the joint, followed by short wide pole. Effect is negligible at initial contact and beyond terminal stance phase (beyond 75% to 100% stance cycle). In general it has been observed that wide pole configuration is more effective in reducing loading effect while a longer pole length helps in negotiating increase in speed. Walking with poles transfers a portion of ground reaction force through the arm supports which effectively offloads the knee joint and can be beneficial in minimizing further damage to the articular surface for OA subject. Effect of increased speed is much more profound in hip loading compared to knee joint, pointing the importance of analyzing adjacent joint dynamics during any pathophysiological evaluation of a particular joint. The results, though insightful has the drawback of drawing conclusion based on a single subject data. Although reported metrics are averaged over 5 gait cycles, multiple user data would help to confirm the observed trends. Another constraint is use of residual actuators to balance the BW reaction forces that results in unrealistic force profile at some instances in the gait cycle. This can be corrected by modeling the full body that will readjust BW and create proper force estimation. MSK model itself can be upgraded with an enhanced knee model [24] to capture both medial and lateral load while synergistic muscle behavior along with muscle redundancy [25] can be exploited to incorporate better force estimation.

#### IV. CONCLUSION

In this paper, we present a modified lower limb MSK model with force measuring knee replacement device and estimate tibio-femoral contact force along with knee joint and hip joint loading and associated muscle force distribution for normal post TKA gait as well as four different types of assisted pole gaits. Effect of gait speed variations were also simulated. Use of simulation platform for analyzing joint loads and contact force provides the flexibility to test different combination theoretically, before finding optimal gait configuration for subject specific evaluations. Results indicate that corrective gait using bilateral hiking pole significantly reduces joint loading at mid stance phase, which is an essential requirement for individuals with medial knee OA. Developed model along with the computational analysis can be used to prescribe supported gait alteration to reduce stress on knee implant, as a therapy to Osteoarthritis cases, personalized rehabilitation planning and optimal implant and brace design.

#### REFERENCES

- [1] D. Kumar, K.T. Manal, K.S. Rudolph (2013); Knee joint loading during gait in healthy controls and individuals with knee osteoarthritis, *Osteoarthritis and Cartilage*, vol. 21, pp: 298-305
- [2] Heller, B., Matziolis (2007). Musculoskeletal biomechanics of the knee joint. principles of preoperative planning for osteotomy and joint replacement. *Orthopade* 36, pp: 628-634
- [3] Zhang, Y. and Jordan, J. M. (2010). Epidemiology of osteoarthritis. *Clin Geriatr Med* , pp:355-369
- [4] Farrokhi, G. S.,M(2015). Altered gait characteristics in individuals with knee osteoarthritis and self reported knee instability. *J. Orthop. Sports Phys.* 45, pp: 351-359.
- [5] Briem, K., Snyder-Mackler, L.(2009). Proximal gait adaptations in medial knee OA. *Journal of Orthopaedic Research*, vol:27(1), pp: 78-83.
- [6] Kemp G, Crossley KM, Wrigley TV, Metcalf BR, Hinman RS. Reducing joint loading in medial knee osteoarthritis: shoes and canes. *Arthritis and Rheumatism*. 2008; vol:59, pp:609-614.
- [7] Mndermann A, Dyrby C, Hurwitz DE, Sharma L, Andriacchi TP. Potential strategies to reduce medial compartment loading in patients with knee osteoarthritis of varying severity. *Arthritis and Rheumatism*. 2004; vol:50, pp: 1172-1178.
- [8] Jonathan P. Walter, Nuray Korkmaz, Benjamin J. Fregly, Marcus G. Pandy, (2015), Contribution of Tibiofemoral Joint Contact to Net Loads at the Knee in Gait; *Orthopaedic Research Society*. Published by Wiley Periodicals, Inc.
- [9] Pellegrini B, Boccia G, Zoppirolli C, Rosa R, Stella F, Bortolan L, et al. (2018) Muscular and metabolic responses to different Nordic walking techniques, when style matters. *PLoS ONE* 13(4)
- [10] Kazemi, D. and Li (2013). Recent advances in computational mechanics of the human knee joint. *262 Comput.Math. Methods Med.* 718423. doi:10.1155/2013/718423
- [11] Huiskes, R. and Chao, E. (1983). A survey of finite element analysis in orthopedic biomechanics: the first 253 decade. *Journal of Biomechanics*, vol: 16, pp:385-409
- [12] E. A. Lingard, J. N. Katz, E. A. Wright, and C. B. Sledge (2004), Predicting the outcome of total knee arthroplasty, *The Journal of Bone & Joint Surgery American Volume*, vol. 86(10), pp.2179-2186, 2004.
- [13] Tien Tuan Dao and Philippe Pouletaut (2015), A Hertzian Integrated Contact Model of the Total Knee Replacement Implant for the Estimation of Joint Contact Forces, *Hindawi Publishing Corporation Journal of Computational Medicine* Article ID 945379,
- [14] A. Erdemir, S. McLean, W. Herzog, and A. J. van den Bogert (2007), Model-based estimation of muscle forces exerted during movements, *Clinical Biomechanics*, vol. 22 (2), pp. 131-154.
- [15] Y.-C. Lin, J. P.Walter, S. A. Banks, M. G. Pandy, and B. J. Fregly (2010), Simultaneous prediction of muscle and contact forces in the knee during gait, *Journal of Biomechanics*, vol. 43(5), pp. 945-952.
- [16] B. J. Fregly, T. F. Besier, D. G. Lloyd (2012), Grand challenge competition to predict in vivo knee loads, *Journal of Orthopaedic Research*, vol. 30 (4), pp. 503-513.
- [17] Benjamin J. Fregly, Darryl D. D'Limab, and Clifford W. Colwell Jr (2009), Effective Gait Patterns for Offloading the Medial Compartment of the Knee, *J Orthop Res*; vol: 27(8), pp: 1016-1021. doi:10.1002/jor.20843.
- [18] S.Delp, F.Anderson, A.Arnold, P.Loan, A.Habib, and D.Thelen (2007), Open-Source Software to Create and Analyze Dynamic Simulations of Movement, *IEEE Transaction on biomedical engineering*, vol. 54(11), pp:1940-50.
- [19] D.Thelen (2003), Adjustment of muscle mechanics model parameters to simulate dynamic contractions in older adults, *J Biomech Eng*, vol.125(1), pp:70-77.
- [20] Katherine M. Steele, Matthew S. DeMers, Michael S. Schwartz, and Scott L. Delp (2012), Compressive Tibiofemoral Force during Crouch Gait, *Gait Posture*; vol: 35(4), pp: 556-560. doi:10.1016/j.gaitpost.2011.11.023.
- [21] Guo M, Axe MJ, Manal K (2007), The Influence of foot progression angle on the knee adduction moment during walking and stair climbing in pain free individuals with knee osteoarthritis. *Gait and Posture*, vol: 26, pp: 436-441. [PubMed: 17134902]
- [22] Yuenyongviwat, V., Duangmanee, S., Iamthanaporn, K. et al (2020). Effect of hip abductor strengthening exercises in knee osteoarthritis: a randomized controlled trial. *BMC Musculoskelet Disord*, vol:21(284).
- [23] Allison L. Kinney, Thor F. Besier, Amy Silder, Scott L. Delp, Darryl D. DLima, and Benjamin J. Fregly (2013), Changes in In Vivo Knee Contact Forces through Gait Modification; *J Orthop Res.*; 31(3): pp:434-440. doi:10.1002/jor.22240.
- [24] O.Mazumder A. Sinha. M. Poduval.etal, (2019). Musculoskeletal modeling to predict and reduce anterior cruciate ligament injury during single leg drop jump activity: Synergistic muscle co-activation approach. In *Annu Int Conf IEEE Eng Med Biol Soc . (IEEE)*, pp: 4108-4112
- [25] O.Mazumder, A. Sinha, A Rai (2020). Muscle synergy control during hand reach task on varying shoulder configuration. In *Annu Int Conf IEEE Eng Med Biol Soc .(IEEE)*, pp: 4839-4843.